SIAM J. SCI. COMPUT.
Vol. 37, No. 6, pp. B1002–B1025




# SHAPE OPTIMIZATION OF AN ELECTRIC MOTOR SUBJECT TO NONLINEAR MAGNETOSTATICS*

P. GANGL†, U. LANGER‡, A. LAURAIN§, H. MEFTAHI§, AND K. STURM¶

**Abstract.** The goal of this paper is to improve the performance of an electric motor by modifying the geometry of a specific part of the iron core of its rotor. To be more precise, the objective is to smooth the rotation pattern of the rotor. A shape optimization problem is formulated by introducing a tracking-type cost functional to match a desired rotation pattern. The magnetic field generated by permanent magnets is modeled by a nonlinear partial differential equation of magnetostatics. The shape sensitivity analysis is rigorously performed for the nonlinear problem by means of a new shape-Lagrangian formulation adapted to nonlinear problems.

**Key words.** shape optimization, nonlinear partial differential equations, magnetostatics, electric motor

**AMS subject classifications.** 49Q10, 49Q12, 65N30, 78A30, 78A55

**DOI.** 10.1137/15100477X

## 1. Introduction.

Advanced shape optimization techniques have become a key tool for the design of industrial structures. In the automotive and aeronautics industries, for instance, the reduction of the drag or of the noise is an important feature which can be reduced by changing the design of the vehicles. In general, when considering a complex mechanical assemblage, it is often possible to optimize the geometry of certain pieces to improve the overall performance of the object. In the industrial sector, the shape optimization of electrical machines is the most economical approach to improve their efficiency and performance. Shape optimization problems are usually formulated as the minimization of a given cost function, with typical examples being the weight or the compliance for elastic systems. The most interesting and challenging problems of these types have linear or nonlinear partial differential equation (PDE) constraints; see, for instance, [1, 10, 12, 17, 18, 21, 22, 26, 33, 34, 35, 36, 45, 46, 48] and the references therein.

In this work, a shape optimization approach is used to improve the design of an electric motor in order to match a desired smoother rotation pattern. As a model

*Submitted to the journal's Computational Methods in Science and Engineering section January 20, 2015; accepted for publication (in revised form) September 24, 2015; published electronically December 22, 2015. The research of the first and second authors was supported by the Austrian Science Fund (FWF) via the Doctoral Program DK W1214 (project DK4) on Computational Mathematics and by the Linz Center of Mechatronics (LCM), which is a part of the COMET K2 program of the Austrian Government.

http://www.siam.org/journals/sisc/37-6/100477.html

†Doctoral Program Computational Mathematics, Johannes Kepler University Linz, Altenberger Straße 69, A-4040 Linz, Austria (peter.gangl@dk-compmath.jku.at).

‡Institute of Computational Mathematics, Johannes Kepler University Linz, Altenberger Straße 69, A-4040 Linz, Austria, and RICAM, Austrian Academy of Sciences, Altenberger Straße 69, 4040 Linz, Austria (ulrich.langer@ricam.oeaw.ac.at).

§Department of Mathematics, Technical University of Berlin, Straße des 17, 10623 Berlin, Germany (laurain@math.tu-berlin.de, meftahi@math.tu-berlin.de). The research of these authors was supported by the DFG Research Center Matheon "Mathematics for key technologies" through the MATHEON-Project C37 "Shape/Topology optimization methods for inverse problems."

¶Department of Mathematics, University of Duisburg-Essen, Thea-Leymann-Straße 9, D-45127 Essen, Germany (kevin.sturm@uni-due.de). The research of this author was supported by the DFG Research Center Matheon through the MATHEON-Project C11.

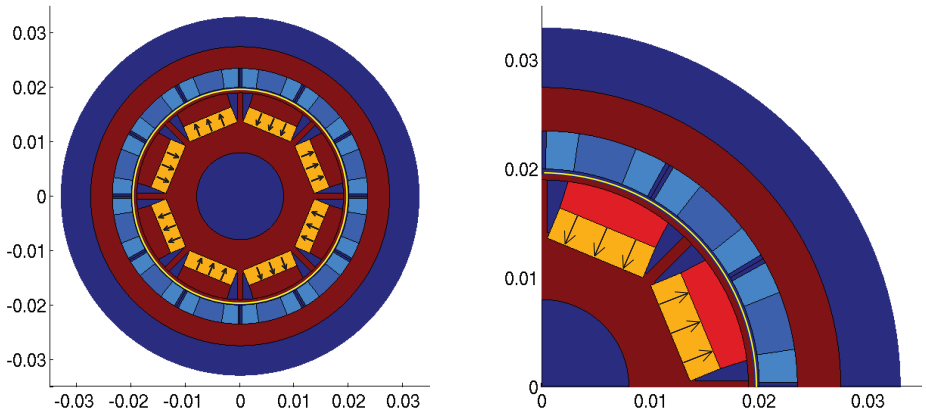


(a) (b)

FIG. 1. (a) *Geometry of the electric motor with permanent magnet areas* $\Omega_{ma}$ *(orange with arrows indicating the directions of magnetization), ferromagnetic material* $\Omega_f^{ref}$ *(brown), coil areas* $\Omega_c$ *(light blue), air* $\Omega_a$ *(dark blue), and thin air gap (yellow layer between rotor and stator);* $\Gamma_0$ *is a circle located in the air gap.* (b) *Zoom on the upper-right quarter of the motor, where the reference design area* $\Omega^{ref} \subset \Omega_f^{ref}$ *corresponds to the highlighted (red) region. The reference region* $\Omega^{ref}$ *is subject to the shape optimization procedure.*

problem, we consider an interior permanent magnet (IPM) brushless electric motor consisting of a rotor (inner part) and a stator (outer part) separated by a thin air gap and both containing an iron core; see Figure 1 for a description of the geometry. The rotor contains permanent magnets. The coil areas are located on the inner part of the stator. In general, inducing current in the coils initiates movement of the rotor due to the interaction between the magnetic fields generated by the electric current and by the magnets. In our application, we are only interested in the magnetic field $B$ for a fixed rotor position without any current induced. Since the magnetic properties of copper in the coils and of air are similar, we model these regions as air regions, too. We refer the reader to [8, 24, 38, 39] for other approaches to the design optimization of IPM electric motors and to [51] for a special method of modeling IPM motors using radial basis functions.

Due to practical restrictions, only some specific parts of the geometry can be modified. In our application, we identify a design subregion $\Omega$ of the iron core of the rotor subject to the shape optimization process. Our objective is to modify $\Omega$ in order to match a desired rotation pattern as well as possible. Practically, this is achieved by tracking a certain desired profile of the magnetic flux density, which is done by reformulating the problem as a shape optimization problem by introducing a tracking-type cost function.

The shape optimization of $\Omega$ has been considered in [14] from the point of view of the topological sensitivity [41, 47]. However, the derivation of the so-called *topological derivative* for nonlinear problems is formal since the mathematical theory for these problems is still in its early stages; see [5, 13, 25] for a few results in this direction. Moreover, the drawback of the topological derivative is that it usually creates geometries with jagged contours.

In this paper, we focus on the shape optimization of the design domain $\Omega$ by

means of the *shape derivative*, which, contrary to the topological derivative, proceeds by smooth deformation of the boundary of a reference design. In this way, the optimal shape has a smooth boundary provided that the numerical algorithm is carefully devised. Computing the shape derivative for problems depending on linear PDEs is a well-understood topic; see, for instance, [10, 20, 48]. For nonlinear problems, the literature is scarcer and the computation of the shape derivative is often formal. A novel aspect of this paper is that it provides an efficient and rigorous way to compute the shape derivative of the cost functional without the need for computing the material derivative of the solution of the nonlinear state equation. The method is based on a novel Lagrangian method for nonlinear problems and on the volume expression of the shape derivative; see [36, 49]. This allows us to obtain a smooth deformation field used as a descent direction in a gradient method. In the numerical algorithm, the interface is updated iteratively using this vector field until it reaches an equilibrium state.

There are actually several methods available to prove the shape differentiability of functions depending on the solution of a PDE without the need for computing the derivative of the state. Several Lagrangian-type methods have been proposed in shape optimization. The approach of Céa [6] is frequently used to derive the formulas for the shape derivative, but it is formal and may lead to the wrong formulas if not used carefully; see [42]. The minimax approach of [9] was the first Lagrangian method with a rigorous mathematical treatment, but it is valid only for semiconvex cost functions. The result described in our paper generalizes that in [9] and simplifies the assumptions, as we can treat nonlinear PDEs and more general cost functionals, whereas the result in [42] only allows dealing with linear PDEs, and therefore our result fills a gap in the literature on Lagrangian methods in shape optimization. Lagrangian approaches also have the advantage of directly providing the adjoint equation. Variational methods have also been proposed recently [27, 30, 31]. In these papers, a rearrangement technique is used to bypass the computation of the shape derivative of the state equation, which allows one to reduce the regularity assumptions. The method proposed in our paper and the methods proposed in [27, 30, 31] are very general, as they require little regularity assumptions on the domains and the solutions of the PDE involved. The approaches to compute the shape derivatives are quite different and it is not yet clear what is the exact relation between these methods.

Another interesting aspect of our paper is that we use a volume expression of the shape derivative instead of the more commonly used boundary expression; i.e., we express the shape derivative as a volume integral instead of a boundary integral. Recent results have shown that the volume expression is advantageous for numerical implementation. In [23] it is shown that the volume expression is more accurate than the boundary representation from a numerical point of view. Indeed, functions such as gradients of the state and adjoint state appearing in the distributed shape derivative need only be defined at grid points and not on the interface. Therefore, one avoids interpolation of these irregular terms. This is particularly useful for transmission problems, where the boundary representation requires one to compute the jump of a function over the interface—a delicate and error-prone operation from the numerical point of view. Another advantage pointed out in [3] is that the discretization process and the shape differentiation commute for the volume expression but not for the boundary expression; i.e., a discretization of the boundary expression of the shape derivative does not generally lead to the same expression as the shape derivative computed when the problem is first discretized. Also, the volume expression is easier to implement, and in certain cases it can be useful to obtain the perturbation field on

the entire domain as in the level set method; see [36].

The rest of the paper is organized as follows. In section 2, we formulate the shape optimization problem and give the underlying nonlinear magnetostatic equation. Existence of a solution to the shape optimization problem is shown in section 3. In section 4, we introduce the general notion of a shape derivative and give an abstract differentiability result which is used later on to compute the shape derivative of the cost functional. Section 5 deals with the shape derivative of the cost functional. Finally, in section 6, a numerical algorithm is presented to optimize the design of $\Omega$, and numerical results showing the optimal shape are presented.

**2. Problem formulation.** Let $D \subset \mathbf{R}^2$ be the smooth bounded domain representing an IPM brushless electric motor as depicted in Figure 1 with a ferromagnetic part $\Omega_f^{\mathrm{ref}} \subset D$, permanent magnets $\Omega_{\mathrm{ma}} \subset D$, air regions $\Omega_a \subset D$, and coil areas $\Omega_c$. The design domain $\Omega$ is included in a reference domain $\Omega^{\mathrm{ref}} \subset \Omega_f^{\mathrm{ref}}$. The inner part of the motor is called the rotor and the outer part the stator. They are separated by a small air gap, shown by the thin yellow circular layer in Figure 1. By $\Gamma_0$ we denote a circle within the air gap. When an electric current is induced in the coils, the rotor containing the permanent magnets rotates. In reality the motor is a three-dimensional object, but considering the problem only on the cross-section of the motor is a modeling assumption that is commonly used; see [2, 4]. For a comparison between two- and three-dimensional models of electric motors, see [32, 50].

Denote by $\Gamma := \partial\Omega$ the boundary of the optimized part $\Omega$, which is assumed to be Lipschitz. We introduce the variable ferromagnetic set $\Omega_f := (\Omega_f^{\mathrm{ref}} \setminus \Omega^{\mathrm{ref}}) \cup \Omega$ and its boundary $\Gamma_f := \partial\Omega_f$. The permanent magnets create a magnetic field in $D$. In our application, we assume the coils to be switched off. Thus, no electric current is induced and the rotor is not moving. For $(x, \zeta) \in D \times \mathbf{R}$, we define the nonlinear, piecewise smooth function $\beta = \beta_\Omega$ as

$$\begin{aligned}\beta_\Omega(x,\zeta) &:= \beta_1(\zeta)\chi_{\Omega_f}(x) + \beta_2(\zeta)\chi_{D\setminus\Omega_f}(x)\\ &= \beta_1(\zeta)(\chi_\Omega(x) + \chi_{\Omega_f^{\mathrm{ref}}\setminus\Omega^{\mathrm{ref}}}(x)) + \beta_2(\zeta)(\chi_{D\setminus\Omega_f^{\mathrm{ref}}}(x) + \chi_{\Omega^{\mathrm{ref}}\setminus\Omega}(x)),\end{aligned}$$

where $\chi$ is the indicator function of a given set. Note that the expression above is meaningful since $\Omega \subset \Omega^{\mathrm{ref}} \subset \Omega_f^{\mathrm{ref}}$. The function $\beta_\Omega$ is related to the magnetic reluctivity $\nu$ as

$$\beta_\Omega(x, \zeta^2) = \nu(x, \zeta),$$

and $\beta_1$ and $\beta_2$ represent the material behavior of the ferromagnetic part $\Omega_f$ and its complement $D \setminus \Omega_f$, respectively. The magnetic field generated by the permanent magnets can be calculated via a boundary value problem of the form

$$\begin{aligned} -\operatorname{div}(\beta_\Omega(x, |\nabla u|^2)\nabla u) &= f \quad \text{in } \Omega_f \text{ and } D \setminus \Omega_f,\\ u &= 0 \quad \text{on } \partial D,\end{aligned} \tag{2.1}$$

with the transmission conditions on the interface $\Gamma_f$,

$$\begin{aligned} [\![u]\!] &= 0 \quad \text{on } \Gamma_f,\\ [\![\beta_\Omega(x, |\nabla u|^2)\partial_n u]\!] &= 0 \quad \text{on } \Gamma_f,\end{aligned} \tag{2.2}$$

where $n$ denotes the outward unit normal vector to $\Omega_f$. Defining by $v^-$ the restriction of some function $v$ on $\Omega_f$ and by $v^+$ its restriction on $D \setminus \Omega_f$, we denote by $[\![v]\!]$ the

jump of $v$ across the interface $\Gamma_f$, i.e.,

$$[\![v]\!] = v^+|_{\Gamma_f} - v^-|_{\Gamma_f}.$$

The weak form of (2.1) reads

$$\text{(2.3)}\quad \text{find } u \in H_0^1(D) \text{ such that } \int_D \beta_\Omega(x, |\nabla u|^2)\nabla u \cdot \nabla v \,\mathrm{d}x = \langle f, v\rangle \quad \forall v \in H_0^1(D),$$

where $\langle \cdot, \cdot \rangle$ denotes the duality bracket between $H^{-1}(D)$ and $H_0^1(D)$. The scalar function $u$ is the third component of the vector potential of the magnetic flux density in three dimensions, $B = \mathrm{curl}((0, 0, u)^T)$. In our model, we consider the restriction of $B$ to a two-dimensional cross-section since the third component vanishes.

In what follows, we make the following assumption for $\beta_1$ and $\beta_2$.

*Assumption* 1. The functions $\beta_1, \beta_2 : \mathbf{R} \to \mathbf{R}$ satisfy the following conditions:

(1) There exist constants $c_1, c_2, c_3, c_4 > 0$ such that

$$c_1 \le \beta_1(\zeta) \le c_2, \quad c_3 \le \beta_2(\zeta) \le c_4 \quad \forall\, \zeta \in \mathbf{R}.$$

(2) The function $s \mapsto \beta_i(s^2)s$ is strongly monotone with monotonicity constant $m$ and Lipschitz continuous with Lipschitz constant $L$:

$$(\beta_i(s^2)\, s - \beta_i(t^2)\, t)\,(s - t) \ge m(s - t)^2 \quad \forall\, s, t \ge 0,$$
$$|\beta_i(s^2)\, s - \beta_i(t^2)\, t| \le L|s - t| \quad \forall\, s, t \ge 0.$$

(3) The functions $\beta_1, \beta_2$ are in $C^1(\mathbf{R})$.

(4) There exist constants $\lambda, \Lambda > 0$ such that for $i = 1, 2$,

$$\lambda|\eta|^2 \le \beta_i(|\rho|^2)|\eta|^2 + 2\beta_i'(|\rho|^2)(\eta \cdot \rho)^2 \le \Lambda|\eta|^2 \quad \forall\, \eta, \rho \in \mathbf{R}^2.$$

The task is to modify the shape of the design region $\Omega \subset \Omega^{\mathrm{ref}}$ in such a way that the radial component of the resulting magnetic flux density on the circle $\Gamma_0$ in the air gap fits a given set of data as well as possible. We consider the following minimization problem:

$$\text{(2.4)}\quad \begin{cases} \text{Minimize } J(\Omega, u) := \displaystyle\int_{\Gamma_0} |B_r(u) - B_d|^2 \mathrm{d}s \\ \text{subject to } \Omega \in \mathcal{O} \text{ and } u \text{ solution of (2.3)}, \end{cases}$$

where

$$\text{(2.5)}\quad \mathcal{O} = \left\{\Omega \subset \Omega^{\mathrm{ref}} \subset \Omega_f^{\mathrm{ref}}, \Omega \text{ open, Lipschitz with uniform Lipschitz constant } L_{\mathcal{O}}\right\}$$

and $\Gamma_0 \subset D$ is a smooth one-dimensional subset of $D$. The sets $\Omega^{\mathrm{ref}}$ and $\Omega_f^{\mathrm{ref}}$ are reference domains; see Figure 1. Here $B_r(u) = \nabla u \cdot \tau$, where $\tau$ is the tangential vector to $\Gamma_0$ and $B_d \in C^1(\Gamma_0)$ denotes the given desired radial component of the magnetic flux density along the air gap. In order to obtain the first-order optimality conditions for this minimization problem, we compute the derivative of $J$ with respect to the shape $\Omega$.

*Remark* 1. Let us note that

- in our application, the right-hand side $f$ represents the magnetization of the permanent magnets. In general, it can be a combination of magnetization and impressed currents in the coils.

- as mentioned above, the link between $\beta_\Omega$ and the magnetic reluctivity is $\beta_\Omega(\cdot,\zeta^2)=\nu(\cdot,\zeta)$. In this case, the boundary value problem (2.1) is called the two-dimensional magnetostatic boundary value problem; see [28, 44]. We will see in section 6 that Assumption 1 is satisfied for $\nu$ due to physical properties.
- the Dirichlet condition $u|_{\partial D}=0$ implies $B\cdot n=0$, and thus no magnetic flux can leave the computational domain $D$.

Given Assumption 1, we can state existence and uniqueness of a solution $u$ to the state equation (2.3).

THEOREM 2.1. *Assume that Assumption* 1(1),(2) *hold. Then problem* (2.3) *admits a unique solution* $u\in H_0^1(D)$ *for any fixed right-hand side* $f\in H^{-1}(D)$, *and we have the estimate*

$$\|u\|_{H_0^1(D)}\le c\|f\|_{H^{-1}(D)}.$$

*Proof.* A proof can be found in [19, 43, 52]. ∎

**3. Existence of optimal shapes.** In this section, we prove that problem (2.4) has a solution $\Omega^\star$ in the set of admissible solutions $\mathcal{O}$ defined by (2.5). We make use of the following result [20, Theorem 2.4.10].

THEOREM 3.1. *Let* $\Omega_n$ *be a sequence in* $\mathcal{O}$. *Then there exists* $\Omega\in\mathcal{O}$ *and a subsequence* $\Omega_{n_k}$, *which converges to* $\Omega$ *in the sense of Hausdorff and of characteristic functions. In addition,* $\overline{\Omega}_{n_k}$ *and* $\partial\Omega_{n_k}$ *converge in the sense of Hausdorff, respectively, towards* $\overline{\Omega}$ *and* $\partial\Omega$.

Let $\Omega_n\in\mathcal{O}$ be a minimizing sequence for problem (2.4). According to Theorem 3.1, we can extract a subsequence, which we still denote by $\Omega_n$, which converges to some $\Omega\in\mathcal{O}$. Denote by $u_n$ and $u$ the solutions of (2.1)–(2.2) with $\Omega_n$ and $\Omega$, respectively. We prove that $u_n\to u$ in $H_0^1(D)$.

First, in view of Theorem 2.1, we have

$$\|u_n\|_{H_0^1(D)}\le c\|f\|_{H^{-1}(D)}, \tag{3.1}$$

where $c$ depends only on $D$. Thus we may extract a subsequence $u_n$ such that $u_n\to u^\star$ in $L^2(D)$ and $\nabla u_n\rightharpoonup\nabla u^\star$ weakly in $L^2(\Omega)$. Extracting yet another subsequence, we may as well assume that $\Omega_n\to\Omega^\star$ in the sense of characteristic functions by applying Theorem 3.1.

Subtracting the variational formulation for two elements $u_n$ and $u_m$ of the sequence and choosing the test function $v=u_n-u_m$, we get

$$\int_D\big(\beta_{\Omega_n}(x,|\nabla u_n|^2)\nabla u_n-\beta_{\Omega_m}(x,|\nabla u_m|^2)\nabla u_m\big)\cdot\nabla(u_n-u_m)\,\mathrm{d}x=0. \tag{3.2}$$

Let us introduce for simplicity the notation $\beta_1^n:=\beta_1(|\nabla u_n|^2)$ and $\beta_2^n:=\beta_2(|\nabla u_n|^2)$. Then, (3.2) becomes

$$\begin{aligned}&\int_D(\beta_1^n(\chi_{\Omega_n}+\chi_{\Omega_f^{\mathrm{ref}}\setminus\Omega^{\mathrm{ref}}})+\beta_2^n(\chi_{D\setminus\Omega_f^{\mathrm{ref}}}+\chi_{\Omega^{\mathrm{ref}}\setminus\Omega_n}))\nabla u_n\cdot\nabla(u_n-u_m)\\&-(\beta_1^m(\chi_{\Omega_m}+\chi_{\Omega_f^{\mathrm{ref}}\setminus\Omega^{\mathrm{ref}}})+\beta_2^m(\chi_{D\setminus\Omega_f^{\mathrm{ref}}}+\chi_{\Omega^{\mathrm{ref}}\setminus\Omega_m}))\nabla u_m\cdot\nabla(u_n-u_m)\,\mathrm{d}x=0.\end{aligned}$$

This yields

$$I_1+I_2+I_3+I_4+I_5+I_6=0, \tag{3.3}$$

where

$$
\begin{aligned}
I_1 &:= \int_D (\chi_{\Omega_n} - \chi_{\Omega_m})\beta_1^n \nabla u_n \cdot \nabla(u_n - u_m)\,dx,\\
I_2 &:= \int_D \chi_{\Omega_m}(\beta_1^n \nabla u_n - \beta_1^m \nabla u_m) \cdot \nabla(u_n - u_m)\,dx,\\
I_3 &:= \int_D \chi_{\Omega_f^{\mathrm{ref}}\setminus\Omega^{\mathrm{ref}}}(\beta_1^n \nabla u_n - \beta_1^m \nabla u_m) \cdot \nabla(u_n - u_m)\,dx,\\
I_4 &:= \int_D \chi_{D\setminus\Omega_f^{\mathrm{ref}}}(\beta_2^n \nabla u_n - \beta_2^m \nabla u_m) \cdot \nabla(u_n - u_m)\,dx,\\
I_5 &:= \int_D (\chi_{\Omega^{\mathrm{ref}}\setminus\Omega_n} - \chi_{\Omega^{\mathrm{ref}}\setminus\Omega_m})\beta_2^n \nabla u_n \cdot \nabla(u_n - u_m)\,dx,\\
I_6 &:= \int_D \chi_{\Omega^{\mathrm{ref}}\setminus\Omega_m}(\beta_2^n \nabla u_n - \beta_2^m \nabla u_m) \cdot \nabla(u_n - u_m)\,dx.
\end{aligned}
$$

To estimate the above integrals, we use the following lemma, which is proven in [43].

LEMMA 3.2. *Let $p, q \in \mathbf{R}^2$. If Assumption* 1(2) *holds, then*

$$[\beta_i(|p|^2)p - \beta_i(|q|^2)q] \cdot (p - q) \geq m|p - q|^2.$$

Applying Lemma 3.2 with $p = \nabla u_n$ and $q = \nabla u_m$, we get

$$
\begin{aligned}
I_2 + I_3 + I_4 + I_6 &\geq m \int_D (\chi_{\Omega_m} + \chi_{\Omega_f^{\mathrm{ref}}\setminus\Omega^{\mathrm{ref}}} + \chi_{D\setminus\Omega_f^{\mathrm{ref}}} + \chi_{\Omega^{\mathrm{ref}}\setminus\Omega_m})|\nabla u_n - \nabla u_m|^2\,dx\\
&= m \int_D |\nabla u_n - \nabla u_m|^2\,dx. \qquad (3.4)
\end{aligned}
$$

Hölder's inequality yields

$$|I_1| \leq \|\beta_1^n\|_{L^\infty(D)} \|\chi_{\Omega_n} - \chi_{\Omega_m}\|_{L^r(D)} \|\nabla u_n\|_{L^2(D)} \|\nabla(u_n - u_m)\|_{L^s(D)},$$

with $r^{-1} + s^{-1} = 1/2$, $r, s \geq 1$. Performing a similar estimate for $I_5$, and in view of Assumption 1(1), this yields

$$|I_1| \leq c_2 \|\chi_{\Omega_n} - \chi_{\Omega_m}\|_{L^r(D)} \|\nabla u_n\|_{L^2(D)} \|\nabla(u_n - u_m)\|_{L^s(D)}, \qquad (3.5)$$

$$|I_5| \leq c_4 \|\chi_{\Omega_n} - \chi_{\Omega_m}\|_{L^r(D)} \|\nabla u_n\|_{L^2(D)} \|\nabla(u_n - u_m)\|_{L^s(D)}. \qquad (3.6)$$

Using equality (3.3) and inequalities (3.1), (3.4), (3.5), (3.6), we obtain the estimate

$$\int_D |\nabla u_n - \nabla u_m|^2\,dx \leq c \|\chi_{\Omega_n} - \chi_{\Omega_m}\|_{L^r(D)} \|f\|_{H^{-1}(D)} \|\nabla(u_n - u_m)\|_{L^s(D)}.$$

Since $\chi_{\Omega_n}$ is a characteristic function, the parameter $r$ can be chosen arbitrarily large, and, consequently, $s$ can be chosen arbitrarily close to 2. Therefore, assuming a little more regularity than $H^1$ for the solution of (2.3), the convergence of the characteristic functions of $\Omega_n$ in $L^p(D)$ implies the strong convergence of $u_n$ towards $u^\star$ in $H_0^1(D)$. Thus, we obtain the following result.

PROPOSITION 3.3. *Let $\Omega_n \in \mathcal{O}$ be a minimizing sequence for problem* (2.4)*, and let $\Omega$ be an accumulation point of this sequence as in Theorem* 3.1*. Assume there exists $\varepsilon > 0$ such that the solution $u$ of* (2.3) *satisfies*

$$\|u\|_{H^{1+\varepsilon}(D) \cap H_0^1(D)} \leq c,$$

*where $c$ depends only on $f$ and $D$. Then the sequence $u_n \in H_0^1(D)$ corresponding to $\Omega_n$ converges to $u$ strongly in $H_0^1(D)$, where $u$ is the solution of (2.3) in $\Omega$.*

*Proof.* We have seen that there exists $u^\star \in H_0^1(D)$ such that $u_n \to u^\star$ in $H_0^1(D)$. We just need to prove that $u^\star = u$. The strong convergence of $u_n$ in $H_0^1(D)$ yields $\nabla u_n \to \nabla u^\star$ pointwise almost everywhere (a.e.) in $D$, and also the pointwise a.e. convergence $\beta_i^n \to \beta_i(|\nabla u^\star|^2)$ for $i = 1, 2$. We also have the pointwise a.e. convergence of the characteristic function $\chi_{\Omega_n}$ to $\chi_{\Omega^\star}$, which implies the pointwise a.e. convergence $\beta_{\Omega_n}(\cdot, |\nabla u_n|^2) \to \beta_{\Omega^\star}(\cdot, |\nabla u^\star|^2)$. Next, the weak formulation for $u_n$ is

$$\int_D \beta_{\Omega_n}(x, |\nabla u_n|^2)\nabla u_n \cdot \nabla v \, \mathrm{d}x = \langle f, v\rangle \quad \forall\ v \in H_0^1(D).$$

The strong convergence of $u_n$ in $H_0^1(D)$ and the pointwise convergence of $\beta_{\Omega_n}(\cdot, |\nabla u_n|^2)$ imply

$$\int_D \beta_{\Omega^\star}(x, |\nabla u^\star|^2)\nabla u^\star \cdot \nabla v \, \mathrm{d}x = \langle f, v\rangle \quad \forall\ v \in H_0^1(D),$$

which finally proves $u^\star = u$. ∎

*Remark* 2. We have in fact proven a stronger result, i.e., the Lipschitz continuity of $\chi_{\Omega_n} \mapsto u_n$ from $L_p(D)$ into $H_0^1(D)$ for some $p \geq 1$.

## 4. Shape derivative.

**4.1. Preliminaries.** In this section, we recall some basic facts about the velocity method in shape optimization used to transform a reference shape; see [10, 48]. In the velocity method, also known as the speed method, a domain $\Omega \subset D \subset \mathbf{R}^2$ is deformed by the action of a velocity field $V$ defined on $D$. Suppose that $D$ is a Lipschitz domain, and denote its boundary by $\Sigma := \partial D$. The domain evolution is described by the solution of the dynamical system

$$\frac{d}{dt}x(t) = V(x(t)), \quad t \in [0, \varepsilon), \qquad x(0) = X \in \mathbf{R}^2 \tag{4.1}$$

for some real number $\varepsilon > 0$. Suppose that $V$ is continuously differentiable and has compact support in $D$, i.e., $V \in \mathcal{D}^1(D, \mathbf{R}^2)$. Then the ordinary differential equation (4.1) has a unique solution on $[0, \varepsilon)$. This enables us to define the diffeomorphism

$$T_t : \mathbf{R}^2 \to \mathbf{R}^2; X \mapsto T_t(X) := x(t). \tag{4.2}$$

With this choice of $V$, the domain $D$ is globally invariant by the transformation $T_t$, i.e., $T_t(D) = D$ and $T_t(\partial D) = \partial D$. For $t \in [0, \varepsilon)$, $T_t$ is invertible. Furthermore, for sufficiently small $\tau > 0$, the Jacobian determinant

$$\xi(t) := \det DT_t \tag{4.3}$$

of $T_t$ is strictly positive. In what follows, we use the notation $DT_t^{-1}$ for the inverse of $DT_t$ and use $DT_t^{-T}$ for the transpose of the inverse. We also denote by

$$\xi_\tau(t) := \xi(t)|DT_t^{-T} n| \tag{4.4}$$

the tangential Jacobian of $T_t$ on $\partial D$.

Then the following lemma holds [10].

LEMMA 4.1. *For $\varphi \in W^{1,1}_{loc}(\mathbf{R}^2)$ and $V \in \mathcal{D}^1(\mathbf{R}^2, \mathbf{R}^2)$ we have*

$$\nabla(\varphi \circ T_t) = DT_t^T(\nabla\varphi) \circ T_t, \qquad \frac{d}{dt}(\varphi \circ T_t) = (\nabla\varphi \cdot V) \circ T_t,$$
$$\frac{d\xi(t)}{dt} = \xi(t)\,[\operatorname{div} V(t)] \circ T_t, \qquad \xi_\tau'(0) = \operatorname{div}_{\partial D} V := \operatorname{div} V|_{\partial D} - DVn \cdot n.$$

DEFINITION 4.2. *Suppose we are given a real valued shape function $J$ defined on a subset $\Xi$ of the power set $2^{\mathbf{R}^2}$. We say that $J$ is Eulerian semidifferentiable at $\Omega \in \Xi$ in the direction $V$ if the following limit exists in $\mathbf{R}$:*

$$dJ(\Omega; V) := \lim_{t \searrow 0} \frac{J(T_t(\Omega)) - J(\Omega)}{t}.$$

*If the map $V \longrightarrow dJ(\Omega; V)$ is linear and continuous with respect to the topology of $\mathcal{D}(D, \mathbf{R}^2) := C_c^\infty(D, \mathbf{R}^2)$, then $J$ is said to be shape differentiable at $\Omega$, and $dJ(\Omega; V)$ is called the shape derivative of $J$.*

**4.2. An abstract differentiability result.** Let $E$ and $F$ be Banach spaces. Let $G$ be a function

$$G : [0, \tau] \times E \times F \to \mathbf{R}, \quad (t, \varphi, \psi) \mapsto G(t, \varphi, \psi) \tag{4.5}$$

that is affine with respect to $\psi$, and define

$$E(t) := \{u \in E |\ d_\psi G(t, u, 0; \hat{\psi}) = 0 \ \forall\ \hat{\psi} \in F\}. \tag{4.6}$$

Let us introduce the following hypotheses.

*Assumption* 2 (condition (H0)). For every $(t, \psi) \in [0, \tau] \times F$, we assume that

(i) the set $E(t)$ is single-valued and we write $E(t) = \{u^t\}$,
(ii) the function $[0, 1] \ni s \mapsto G(t, su^t + s(u^t - u^0), \psi)$ is absolutely continuous,
(iii) the function $[0, 1] \ni s \mapsto d_\varphi G(t, su^t + (1 - s)u^0, \psi; \varphi)$ belongs to $L^1(0, 1)$ for all $\varphi \in E$.

For $t \in [0, \tau]$ and $u^t \in E(t)$, let us introduce the set

$$Y(t, u^t, u^0) := \left\{ q \in F |\ \forall \hat{\varphi} \in E : \int_0^1 d_\varphi G(t, su^t + (1 - s)u^0, q; \hat{\varphi})\, ds = 0 \right\}, \tag{4.7}$$

which is called the solution set of the *averaged adjoint equation* with respect to $t$, $u^t$, and $u^0$. Note that $Y(0, u^0, u^0)$ coincides with the solution set of the usual adjoint state equation:

$$Y(0, u^0, u^0) = \left\{ q \in F |\ d_\varphi G(0, u^0, q; \hat{\varphi}) = 0 \ \forall\ \hat{\varphi} \in E \right\}. \tag{4.8}$$

The following result, proved in [49], allows us to compute the Eulerian semiderivative of Definition 4.2 without computing the material derivative $\dot{u}$. The key is the introduction of the set (4.7).

THEOREM 4.3. *Let condition* (H0) *hold and the following conditions be satisfied:*

(H1) *For all $t \in [0, \tau]$ and all $\psi \in F$, the derivative $\partial_t G(t, u^0, \psi)$ exists.*
(H2) *For all $t \in [0, \tau]$, $Y(t, u^t, u^0)$ is single-valued, and we write $Y(t, u^t, u^0) = \{p^t\}$.*
(H3) *We have*

$$\lim_{t \searrow 0} \frac{G(t, u^0, p^t) - G(0, u^0, p^t)}{t} = \partial_t G(0, u^0, p^0).$$

*Then, for all $\psi \in F$, we obtain*

$$\frac{d}{dt}(G(t,u^t,\psi))|_{t=0} = \partial_t G(0,u^0,p^0). \tag{4.9}$$

**4.3. Adjoint equation.** Introduce the Lagrangian associated to the minimization problem (2.4) for all $\varphi, \psi \in H_0^1(D)$:

$$G(\Omega,\varphi,\psi) := \int_{\Gamma_0} |B_r(\varphi) - B_d|^2 \, ds + \int_D \beta(x,|\nabla\varphi|^2)\nabla\varphi\cdot\nabla\psi \, dx - \langle f,\psi\rangle. \tag{4.10}$$

The adjoint state equation is obtained by differentiating $G$ with respect to $\varphi$ at $\varphi = u$ and $\psi = p$,

$$d_\varphi G(\Omega,u,p;\varphi) = 0 \quad \forall\ \varphi \in H_0^1(D)$$

or, equivalently,

$$\begin{aligned} &2\int_D \partial_\zeta\beta(x,|\nabla u|^2)(\nabla u\cdot\nabla\varphi)(\nabla u\cdot\nabla p)\,dx + \int_D \beta(x,|\nabla u|^2)\nabla p\cdot\nabla\varphi\,dx \\ &= -2\int_{\Gamma_0}(B_r(u)-B_d)B_r(\varphi)\,ds \quad \forall\ \varphi\in H_0^1(D). \end{aligned} \tag{4.11}$$

Introduce the mean curvature $\kappa$ of $\Gamma_0$ and the Laplace–Beltrami operator $\Delta_\tau$ on $\Gamma_0$:

$$\Delta_\tau u := \Delta u - \kappa\frac{\partial u}{\partial n} - \frac{\partial^2 u}{\partial n^2}.$$

Using $B_r(u) = \nabla u\cdot\tau$ as well as the equalities

$$(\nabla u\cdot\nabla\varphi)(\nabla u\cdot\nabla p) = ((\nabla u\otimes\nabla u)\nabla p)\cdot\nabla\varphi,$$
$$\int_{\Gamma_0}(\nabla_\tau u - B_d\,\tau)\cdot\nabla_\tau\varphi\,ds = -\int_{\Gamma_0}\Delta_\tau u\varphi - \mathrm{div}_\tau(B_d\,\tau)\varphi ds$$

and Green's formula, we deduce the corresponding strong form of (4.11),

$$\begin{aligned} -\mathrm{div}(\mathcal{A}_1(\nabla u)\nabla p) &= 0 \quad \text{in } \Omega,\\ -\mathrm{div}(\mathcal{A}_2(\nabla u)\nabla p) &= 0 \quad \text{in } D\setminus\Omega,\\ p &= 0 \quad \text{on } \partial D, \end{aligned} \tag{4.12}$$

with the transmission conditions

$$\begin{aligned} [\![p]\!]_\Gamma &= 0 \quad \text{on } \Gamma,\\ [\![\mathcal{A}(\nabla u)\nabla p\cdot n]\!]_\Gamma &= 0 \quad \text{on } \Gamma,\\ [\![\mathcal{A}(\nabla u)\nabla p\cdot n]\!]_{\Gamma_0} &= 2\,(\Delta_\tau u - \mathrm{div}_\tau(B_d\,\tau)) \quad \text{on } \Gamma_0, \end{aligned} \tag{4.13}$$

where

$$\begin{aligned} \mathcal{A}(\nabla u) &:= \mathcal{A}_1(\nabla u)\chi_\Omega + \mathcal{A}_2(\nabla u)\chi_{D\setminus\Omega},\\ \mathcal{A}_i(\nabla u) &:= \beta_i(|\nabla u|^2)I_2 + 2\partial_\zeta\beta_i(|\nabla u|^2)\nabla u\otimes\nabla u \in \mathbf{R}^{2,2}, \quad i=1,2. \end{aligned}$$

Note that, with this notation, the variational form of the equation can be written as

$$\int_D \mathcal{A}(\nabla u)\nabla p\cdot\nabla\varphi\,dx = -2\int_{\Gamma_0}(B_r(u)-B_d)B_r(\varphi)\,ds \quad \forall\ \varphi\in H_0^1(D). \tag{4.14}$$

Now let us investigate the existence of a solution for the adjoint equation.

THEOREM 4.4. *Let Assumption* 1(4) *hold. For given* $u \in H_0^1(D)$, *the equation*

$$\int_D \mathcal{A}(\nabla u)\nabla p \cdot \nabla \varphi \, dx = -2 \int_{\Gamma_0} (B_r(u) - B_d) B_r(\varphi) \, ds \quad \forall \varphi \in H_0^1(D) \tag{4.15}$$

*has a unique solution* $p \in H_0^1(D)$.

*Proof.* For fixed $u \in H_0^1(D)$, define the bilinear form

$$a'(u;\cdot,\cdot) : H_0^1(D) \times H_0^1(D) \to \mathbb{R},$$
$$(v, w) \mapsto \int_D \mathcal{A}(\nabla u)\nabla v \cdot \nabla w \, dx.$$

We check the conditions of Lax–Milgram's theorem. The ellipticity of the bilinear form $a'(u;\cdot,\cdot)$ can be seen as follows:

$$a'(u; v, v) = \int_D \mathcal{A}(\nabla u)\nabla v \cdot \nabla v \, dx \geq \lambda \int_D |\nabla v|^2 \mathrm{d}x \geq \lambda \, C \|v\|^2_{H^1(D)},$$

where we have used the first estimate in Assumption 1(4) and Poincaré's inequality since $v \in H_0^1(D)$. The boundedness of the bilinear form $a'(u;\cdot,\cdot)$ can be seen by Hölder's inequality and again by Assumption 1(4). The right-hand side is obviously a linear and continuous functional on $H_0^1(D)$,

$$\langle F_u, \varphi \rangle = -2 \int_{\Gamma_0} (B_r(u) - B_d) B_r(\varphi) \, ds,$$

and thus Lax–Milgram's theorem yields the existence of a unique solution $p$ to the variational problem

$$a'(u; \varphi, p) = \langle F_u, \varphi \rangle \quad \forall \, \varphi \in H_0^1(D),$$

which concludes the proof. ∎

**5. Shape derivative of the cost function.** In this section we prove that the cost function $J$ given by (2.4) is shape differentiable in the sense of Definition 4.2. Moreover, we derive a domain expression of the shape derivative. To be more precise, Theorem 4.3 is applied to show Theorem 5.1. Anticipating the application of section 6, we assume in what follows that $f$ has the form

$$f = f_0 + \operatorname{div} M \quad \text{with } M = M_1 \chi_{\Omega_{\mathrm{ma}}}(x) + M_2 \chi_{D \setminus \Omega_{\mathrm{ma}}}(x),$$

where $f_0 \in H^1(D)$.

In this section we assume $\Omega \subset \Omega^{\mathrm{ref}}$, $V \in \mathcal{D}^1(\mathbf{R}^2, \mathbf{R}^2)$, and $\operatorname{supp}(V) \cap \Gamma_0 = \emptyset$. Denote by $\Omega_k^{\mathrm{ref}}$, $k = 1, \ldots, 8$, the connected components of $\Omega^{\mathrm{ref}}$ (see Figure 1). Introduce $\Gamma^{\mathrm{ref}}$, the boundary of $\Omega^{\mathrm{ref}}$. The four sides of $\Gamma^{\mathrm{ref}}$ are denoted $\Gamma_k^{\mathrm{ref},N}, \Gamma_k^{\mathrm{ref},W}, \Gamma_k^{\mathrm{ref},E}, \Gamma_k^{\mathrm{ref},S}$, where the exponents mean north, south, east, and west, respectively. We assume $V \cdot n = 0$ on $\Gamma_k^{\mathrm{ref},S}$ and $V \cdot n \leq 0$ on $\Gamma_k^{\mathrm{ref},E} \cup \Gamma_k^{\mathrm{ref},W} \cup \Gamma_k^{\mathrm{ref},N}$. These conditions guarantee that $\Omega_t := T_t(\Omega) \subset \Omega^{\mathrm{ref}}$. In addition, we assume that the vector field $V$ is such that the transformation $T_t$ satisfies $T_t(\Omega_{\mathrm{ma}}) = \Omega_{\mathrm{ma}}$ for $t$ small enough.

THEOREM 5.1. *Let* $\beta_1$ *and* $\beta_2$ *satisfy Assumption* 1. *Then the functional* $J$ *is*

*shape differentiable, and its shape derivative in the direction $V$ is given by*

$$\begin{aligned} dJ(\Omega;V) = &-\int_D (f_0 \operatorname{div}(V) + \nabla f_0 \cdot V) p \, dx \\ &+ \int_{\Omega_{ma}} \mathbb{P}'(0)\nabla p \cdot M_1 \, dx + \int_{D\setminus\Omega_{ma}} \mathbb{P}'(0)\nabla p \cdot M_2 \, dx \\ &+ \int_D \beta_\Omega(x, |\nabla u|^2)\mathbb{R}'(0)\nabla u \cdot \nabla p \, dx \\ &- \int_D 2\partial_\zeta \beta_\Omega(x, |\nabla u|^2)(DV^T \nabla u \cdot \nabla u)(\nabla u \cdot \nabla p) \, dx, \end{aligned} \tag{5.1}$$

*where $\mathbb{P}'(0) = (\operatorname{div} V)I_2 - DV^T$, $\mathbb{R}'(0) = (\operatorname{div} V)I_2 - DV^T - DV$, $I_2 \in \mathbb{R}^{2,2}$ is the identity matrix, and $u, p \in H_0^1(D)$ are, respectively, the solutions of the problems* (2.1)–(2.2) *and* (4.12)–(4.13).

*Remark* 3. Note that the last integral in (5.1) is well-defined thanks to Assumption 1(4). To see this, note that $V \in C^1(\overline{D}, \mathbf{R}^2)$ and that, for all $\zeta \in \mathbf{R}^2$, we have $\beta'(|\zeta|^2)|\zeta|^2 \le \Lambda$. Hence,

$$\begin{aligned} &\left| \int_D 2\partial_\zeta \beta_\Omega(x, |\nabla u|^2)(DV^T \nabla u \cdot \nabla u)(\nabla u \cdot \nabla p) \, dx \right| \\ &\qquad \le C \int_D \partial_\zeta \beta_\Omega(x, |\nabla u|^2)|\nabla u|^2 |\nabla u \cdot \nabla p| \, dx \\ &\qquad \le C\Lambda \int_D |\nabla u \cdot \nabla p| \, dx < \infty. \end{aligned} \tag{5.2}$$

The other terms in (5.1) are obviously well-defined.

*Proof of Theorem* 5.1. Let us consider the transformation $T_t$ defined by (4.2) with $V \in \mathcal{D}^1(D, \mathbf{R}^2)$. In this case, $T_t(D) = D$, but, in general, $T_t(\Omega) := \Omega_t \ne \Omega$. We define the Lagrangian $G(\Omega_t, \varphi, \psi)$ at the transformed domain $\Omega_t$ for all $\varphi, \psi$ in $H_0^1(D)$ as follows:

$$G(\Omega_t, \varphi, \psi) = \int_{\Gamma_0} |B_r(\varphi) - B_d|^2 \, ds + \int_D \beta_{\Omega_t}(x, |\nabla\varphi|^2)\nabla\varphi \cdot \nabla\psi \, dx - \langle f, \psi \rangle.$$

Since

$$f = f_0 + \operatorname{div} M \quad \text{ with } M = M_1 \chi_{\Omega_{\mathrm{ma}}}(x) + M_2 \chi_{D\setminus\Omega_{\mathrm{ma}}}(x),$$

where $M_1$ and $M_2$ are constant vectors, we transform the last term in $G$ into

$$\langle f, \psi \rangle = \int_D f_0 \psi + \langle \operatorname{div} M, \psi \rangle = \int_D f_0 \psi - \int_D M \cdot \nabla\psi,$$

which yields

$$\begin{aligned} G(\Omega_t, \varphi, \psi) = &\int_{\Gamma_0} |B_r(\varphi) - B_d|^2 \, ds + \int_D \beta_{\Omega_t}(x, |\nabla\varphi|^2)\nabla\varphi \cdot \nabla\psi \, dx \\ &- \int_D f_0 \psi + \int_{\Omega_{\mathrm{ma}}} M_1 \cdot \nabla\psi + \int_{D\setminus\Omega_{\mathrm{ma}}} M_2 \cdot \nabla\psi. \end{aligned}$$

In order to differentiate $G(\Omega_t, \varphi, \psi)$ with respect to $t$, the integrals in $G(\Omega_t, \varphi, \psi)$ need to be transported back to the reference domain $\Omega$ using the transformation $T_t$.

However, composing by $T_t$ inside the integrals creates terms $\varphi \circ T_t$ and $\psi \circ T_t$, which might be nondifferentiable. To avoid this problem, we need to parameterize the space $H_0^1(D)$ by composing the elements of $H_0^1(D)$ with $T_t^{-1}$. Following this argument, we introduce

$$\mathfrak{G}(t,\varphi,\psi) := G(\Omega_t, \varphi \circ T_t^{-1}, \psi \circ T_t^{-1}). \tag{5.3}$$

In (5.3), we proceed to the change of variable $x = T_t(\bar{x})$. This yields

$$\begin{aligned}\mathfrak{G}(t,\varphi,\psi) = &\int_{\Gamma_0} \xi_\tau(t)|B_r(\varphi) - B_d \circ T_t|^2 \, ds \\ &+ \int_D \beta_\Omega(x, |\mathbb{M}(t)\nabla\varphi|^2)\mathbb{M}(t)\nabla\varphi \cdot \mathbb{M}(t)\nabla\psi \, \xi(t) \, dx \\ &- \int_D f_0 \circ T_t \psi \xi(t) \, dx + \int_{\Omega_{\mathrm{ma}}} M_1 \cdot \mathbb{M}(t)\nabla\psi\xi(t) \, dx \\ &+ \int_{D\setminus\Omega_{\mathrm{ma}}} M_2 \cdot \mathbb{M}(t)\nabla\psi \, \xi(t) \, dx,\end{aligned} \tag{5.4}$$

where $\mathbb{M}(t) = DT_t^{-T}$ and $\xi(t), \xi_\tau(t)$ are defined in (4.3) and (4.4), respectively. Note that we have used the assumption $T_t(\Omega_{\mathrm{ma}}) = \Omega_{\mathrm{ma}}$ in the computation of $\mathfrak{G}(t,\varphi,\psi)$.

Observe that $J(\Omega_t) = \mathfrak{G}(t, u^t, \psi)$ for all $\psi \in H_0^1(D)$, where $u^t \in H_0^1(D)$ solves

$$\begin{aligned}&\int_D \beta_\Omega(x, |\mathbb{M}(t)\nabla u^t|^2)\mathbb{M}(t)\nabla u^t \cdot \mathbb{M}(t)\nabla\psi\xi(t) \, dx \\ &\quad = \int_D f_0 \circ T_t \psi\xi(t) \, dx - \int_{\Omega_{\mathrm{ma}}} M_1 \cdot \mathbb{M}(t)\nabla\psi\xi(t) \, dx - \int_{D\setminus\Omega_{\mathrm{ma}}} M_2 \cdot \mathbb{M}(t)\nabla\psi\xi(t) \, dx.\end{aligned} \tag{5.5}$$

To prove Theorem 5.1, we need to check the conditions of Theorem 4.3 for the function $\mathfrak{G}(t,\varphi,\psi)$ with $E = F = H_0^1(D)$.

*Verification of* (H0). Condition (H0)(i) is satisfied since $E(t) = \{u^t\}$, where $u^t \in H_0^1(D)$ is the solution of the state equation (5.5). Conditions (H0)(ii) and (H0)(iii) of Assumption 2 are also satisfied due to the differentiability of the functions $\beta_1, \beta_2$ and Assumption 1.

*Verification of* (H1). Condition (H1) is satisfied since $\mathbb{M}(t)$, $\xi(t)$, and $\xi_\tau(t)$ are smooth.

*Verification of* (H2). $Y(t, u^t, u^0) = \{p^t\}$, where $p^t \in H_0^1(D)$ is the unique solution of

$$\begin{aligned}&\int_0^1 \int_D 2\partial_\zeta \beta_\Omega(x, |\mathbb{M}(t)\nabla u_t^s|^2)((\mathbb{M}(t)\nabla u_t^s \otimes \mathbb{M}(t)\nabla u_t^s)\mathbb{M}(t)\nabla p^t) \cdot \mathbb{M}(t)\nabla\psi\xi(t) \, dx \, ds \\ &\qquad + \int_0^1 \int_D \beta_\Omega(x, |\mathbb{M}(t)\nabla u_t^s|^2)\mathbb{M}(t)\nabla\psi \cdot \mathbb{M}(t)\nabla p^t \xi(t) \, dx \, ds \\ &\quad = -\int_0^1 \int_{\Gamma_0} 2(B_r(u_t^s) - B_d)B_r(\psi)\xi(t) \, dx \, ds \quad \forall \, \psi \in H_0^1(D),\end{aligned} \tag{5.6}$$

where we define $u_t^s := su^t + (1-s)u^0$. This can also be rewritten in a more compact

way as

$$\begin{aligned}\int_0^1 \int_D \mathcal{A}(\mathbb{M}(t)\nabla u_t^s)\mathbb{M}(t)\nabla p^t \cdot \mathbb{M}(t)\nabla\psi\xi(t)\,dx\,ds \\ = -\int_0^1 \int_{\Gamma_0} 2(B_r(u_t^s) - B_d)B_r(\psi)\xi(t)\,dx\,ds.\end{aligned} \tag{5.7}$$

To prove that the previous equation has indeed a unique solution, we first check that all integrals are finite in the previous equation. To verify this, we use Hölder's inequality to obtain

$$\begin{aligned}&\int_D 2\partial_\zeta\beta_\Omega(x,|\mathbb{M}(t)\nabla u_t^s|^2)((\mathbb{M}(t)\nabla u_t^s \otimes \mathbb{M}(t)\nabla u_t^s)\mathbb{M}(t)\nabla p^t)\cdot\mathbb{M}(t)\nabla\psi\xi(t)\,dx \\ &\le c\left(\int_D 2\partial_\zeta\beta_\Omega(x,|\mathbb{M}(t)\nabla u_t^s|^2)(\mathbb{M}(t)\nabla u_t^s\cdot\mathbb{M}(t)\nabla p^t)^2\,dx\right)^{1/2} \\ &\qquad\cdot\left(\int_D 2\partial_\zeta\beta_\Omega(x,|\mathbb{M}(t)\nabla u_t^s|^2)(\mathbb{M}(t)\nabla u_t^s\cdot\mathbb{M}(t)\nabla\psi)^2\,dx\right)^{1/2}\end{aligned}$$

and

$$\begin{aligned}&\int_D \beta_\Omega(x,|\mathbb{M}(t)\nabla u_t^s|^2)\mathbb{M}(t)\nabla\psi\cdot\mathbb{M}(t)\nabla p^t\xi(t)\,dx \\ &\le c\left(\int_D \beta_\Omega(x,|\mathbb{M}(t)\nabla u_t^s|^2)|\mathbb{M}(t)\nabla\psi|^2\,dx\right)^{1/2}\left(\int_D \beta_\Omega(x,|\mathbb{M}(t)\nabla u_t^s|^2)|\mathbb{M}(t)\nabla p^t|^2\,dx\right)^{1/2}.\end{aligned}$$

Adding both equations and using part (4) of Assumption 1, we get

$$\int_D \mathcal{A}(\mathbb{M}(t)\nabla u_t^s)\mathbb{M}(t)\nabla p^t\cdot\mathbb{M}(t)\nabla\psi\xi(t)\,dx\,ds \le c\|\psi\|_{H^1(D)}\|\bar{p}^t\|_{H^1(D)}, \tag{5.8}$$

where the constant $c>0$ is independent of $s$.

The existence of a solution $p^t$ follows from Theorem 4.4. Since $\mathbb{M}(t) = DT_t^{-T}$, there are numbers $C>0$ and $\tau>0$ such that, for all $t\in[0,\tau]$ and $\rho\in\mathbf{R}^2$, we have $\mathbb{M}(t)\rho\cdot\rho \ge C|\rho|^2$. Note that $p^0 = p \in Y(0,u^0,u^0)$ is the unique solution of the adjoint equation (4.12)–(4.13).

*Verification of* (H3). To verify this assumption, we show that there is a sequence $(p^{t_k})_{k\in\mathbf{N}}$, where $\{p^{t_k}\} = Y(t_k,u^{t_k},u^0)$, which converges weakly in $H_0^1(D)$ to the solution of the adjoint equation, and that $(t,\psi)\mapsto\partial_t\mathfrak{G}(t,u^0,\psi)$ is weakly continuous. In order to prove this, we need the following lemmas.

LEMMA 5.2. *Let $m\in\{0,1\}$ and the velocity field $V\in\mathcal{D}^1(\mathbf{R}^2,\mathbf{R}^2)$ be given, and let $\varphi\in H^m(\mathbf{R}^2)$. We denote by $T_t$ the transformation associated to $V$. Then we have*

$$\lim_{t\to0}\varphi\circ T_t = \varphi \text{ and } \lim_{t\to0}\varphi\circ T_t^{-1} = \varphi \quad \text{in } H^m(D).$$

*Proof.* See, for instance, [10]. ∎

Recall that according to Remark 2, there are constants $C,\varepsilon>0$ and $p\ge1$ such that

$$\|u(\chi_1)-u(\chi_2)\|_{H^1(D)} \le C\|\chi_1-\chi_2\|_{L^1(D)}^{1/p} \quad \forall\chi_1,\chi_2\in\Xi(D) \tag{5.9}$$

and

$$\Xi(D) := \{\chi_\Omega : \Omega \subset D \text{ is measurable and } \chi_\Omega(1-\chi_\Omega) = 0 \text{ a.e. in } D\}.$$

With this result it is easy to see that $t \mapsto u^t$ is in fact continuous.

LEMMA 5.3. *Let Assumption* 1(1)–(3) *hold. Then the mapping* $t \mapsto u^t := u_t \circ T_t$ *is continuous from the right at* 0*, i.e.,*

$$\lim_{t \searrow 0} \|u^t - u\|_{H_0^1(D)} = 0.$$

*If in addition Assumption* 1(4) *is satisfied, then there are constants* $c, \tau > 0$ *such that*

$$\|u^t - u\|_{H_0^1(D)} \le tc \quad \forall\, t \in [0,\tau].$$

*Proof.* Since $\|\cdot\|_{H_0^1(D)}$ and the $L^2$-norm of the gradient are equivalent norms on $H_0^1(D)$, it suffices to show $\lim_{t\searrow 0} \|\nabla u^t - \nabla u\|_{L^2(D,\mathbf{R}^d)} = 0$. First, introduce

$$A_t(x) := \xi(t)(D\Phi_t(x))^{-T}(D\Phi_t(x))^{-1},$$

which satisfies $|A_t(x)^{-1}| \le c$ for all $t \in [0,\tau]$, and hence

$$\begin{aligned}\forall x \in \Omega,\, \forall t \in [0,\tau],\, \forall \zeta \in \mathbf{R}^2 :\ |\zeta|^2 &\le |A_t(x)^{-1}|\, |\xi(t)(D\Phi_t(x))^{-T}\zeta \cdot (D\Phi_t(x))^{-T}\zeta|^2 \\ &\le cA_t(x)\zeta\cdot\zeta.\end{aligned}$$

Therefore, for all $f_0 \in H^1(D)$ and all $t \in [0,\tau]$,

$$\int_D |\nabla(f_0 \circ T_t^{-1})|^2\, dx = \int_D A_t \nabla f_0 \cdot \nabla f_0\, dx \ge \frac{1}{c}\int_D |\nabla f_0|^2\, dx.$$

Further, we get from this estimate that for all $t \in [0,\tau]$,

$$c\|f_0\|_{H^1(D)} \le \|f_0 \circ T_t^{-1}\|_{H^1(D)}. \tag{5.10}$$

Now setting $\chi_1 := \chi_\Omega$ and $\chi_2 := \chi_{\Omega_t} = \chi_\Omega \circ T_t^{-1}$ and denoting the corresponding solutions of (2.3) by $u := u(\chi_\Omega)$ and $u_t := u(\chi_{\Omega_t})$, we infer from (5.9) and (5.10) that

$$c\|\nabla(u\circ T_t) - \nabla u^t\|_{L^2(D,\mathbf{R}^d)} \le \|\nabla u - \nabla u_t\|_{L^2(D,\mathbf{R}^d)} \le C\|\chi_\Omega - \chi_\Omega \circ T_t^{-1}\|_{L^1(D)},$$

where $u^t := u_t \circ T_t$. Employing the previous estimates, we get for all $t \in [0,\tau]$

$$\begin{aligned}\|\nabla u - \nabla u^t\|_{L^2(D,\mathbf{R}^d)} &\le \|\nabla u - \nabla(u\circ T_t)\|_{L^2(D,\mathbf{R}^d)} + \|\nabla(u\circ T_t) - \nabla u^t\|_{L^2(D,\mathbf{R}^d)} \\ &\le \tilde{c}\left(\|\nabla u - \nabla(u\circ T_t)\|_{L^2(D,\mathbf{R}^d)} + \|\chi_\Omega - \chi_\Omega \circ T_t^{-1}\|_{L^1(D)}\right).\end{aligned}$$

Finally, taking into account Lemma 5.2, we obtain the desired continuity. The Lipschitz continuity under the additional Assumption 1(4) was shown in [49]. ∎

Using Lemma 5.3 we are able to show the following.

LEMMA 5.4. *The solution* $p^t$ *of* (5.6) *converges weakly in* $H_0^1(D)$ *to the solution* $p$ *of the adjoint equation* (4.12)–(4.13).

*Proof.* The existence of a solution of (5.6) follows from Theorem 4.4. Inserting $\psi = p^t$ as a test function into (5.6), we see that the estimate $\|u^t\|_{H^1(D)} \le C$ implies $\|p^t\|_{H^1(D)} \le C$ for $t$ sufficient small. From the boundedness, we infer that $(p^t)_{t\ge 0}$

converges weakly to some $w \in H_0^1(D)$. In Lemma 5.3 we proved $u^t \to u$ in $H_0^1(D)$, which we can use to pass to the limit in (5.6) and obtain

$$p^{t_k} \rightharpoonup p \quad \text{in } H_0^1(D) \quad \text{for } t_k \to 0 \quad \text{as } k \to \infty,$$

where $p \in H_0^1(D)$ solves the adjoint equation (4.12)–(4.13). By uniqueness we conclude that $w = p$. ∎

Now we proceed to the differentiation of (5.4) at $t > 0$. Introducing the notation $\mathbb{P}(t) = \xi(t)\mathbb{M}(t)$ and $\mathbb{R}(t) := \xi(t)\mathbb{M}(t)^T\mathbb{M}(t)$, we obtain

(5.11)

$$\begin{aligned}
\partial_t \mathfrak{G}(t,\varphi,\psi) &= \int_{\Gamma_0} \xi_\tau'(t)|B_r(\varphi) - B_d \circ T_t|^2 \, ds \\
&\quad - 2\int_{\Gamma_0} \xi_\tau(t)(B_r(\varphi) - B_d \circ T_t)\nabla B_d \circ T_t \cdot V \, ds \\
&\quad + 2\int_D \partial_\zeta \beta_\Omega(x, |\mathbb{M}(t)\nabla\varphi|^2)(\mathbb{M}'(t)\nabla\varphi \cdot \mathbb{M}(t)\nabla\varphi)\mathbb{M}(t)\nabla\varphi \cdot \mathbb{M}(t)\nabla\psi\xi(t) \, dx \\
&\quad + \int_D \beta_\Omega(x, |\mathbb{M}(t)\nabla\varphi|^2)\mathbb{R}'(t)\nabla\varphi \cdot \nabla\psi \, dx \\
&\quad - \int_D f_0 \circ T_t \, \psi\xi'(t) + \nabla f_0 \circ T_t \cdot V \, \psi\xi(t) \, dx \\
&\quad + \int_{\Omega_{\mathrm{ma}}} \mathbb{P}'(t)\nabla\psi \cdot M_1 \, dx + \int_{D\setminus\Omega_{\mathrm{ma}}} \mathbb{P}'(t)\nabla\psi \cdot M_2 \, dx,
\end{aligned}$$

and this shows that for fixed $\varphi \in H_0^1(D)$, the mapping $(t,\psi) \mapsto \partial_t\mathfrak{G}(t,\varphi,\psi)$ is weakly continuous. This finishes the proof that (H3) is satisfied.

Consequently, we may apply Theorem 4.3 and obtain $dJ(\Omega;V) = \partial_t\mathfrak{G}(0,u,p)$, where $u \in H_0^1(D)$ solves the state equation (2.1)–(2.2) and $p \in H_0^1(D)$ is a solution of the adjoint equation (4.12)–(4.13). In order to compute $\partial_t\mathfrak{G}(0,u,p)$, note that the integrals on $\Gamma_0$ vanish due to $V = 0$ on $\Gamma_0$, $\mathbb{M}'(0) = -DV^T$, $\mathbb{P}'(0) = (\operatorname{div} V)I_2 - DV^T$, and $\mathbb{R}'(0) = (\operatorname{div} V)I_2 - DV^T - DV$. Finally, we have proved formula (5.1). This concludes the proof of Theorem 5.1. ∎

**6. Optimization of the rotor core.** In this section, we use the shape derivative derived in Theorem 5.1 to determine the optimal design for the electric motor described in section 2. Recall that the problem consists of finding the shape $\Omega \subset \Omega_f$ of the ferromagnetic subdomain of the electric motor depicted in Figure 1 which minimizes the cost functional

$$J(\Omega) = \int_{\Gamma_0} |B_r(u_\Omega) - B_d|^2 \mathrm{d}s$$

among all admissible shapes $\Omega \in \mathcal{O}$, where $\Gamma_0$ is a circle in the air gap, $B_r(u_\Omega)$ denotes the radial component of the magnetic flux density $B = B(u_\Omega)$ on $\Gamma_0$, and $B_d$ is a given sine curve, $B_d(\theta) = \frac{1}{2}\sin(4\,\theta)$, where $\theta$ denotes the angle in polar coordinates with origin at the center of the motor; see Figure 1. Minimizing this functional leads to a reduction of the total harmonic distortion (THD) (see [4, 7]) of the flux density, which causes the rotor to rotate more smoothly. Here, $u_\Omega$ is the solution of the two-dimensional magnetostatic boundary value problem, the weak form of which reads as follows:

(6.1) Find $u \in H_0^1(D)$ such that $\displaystyle\int_D \nu(x,|\nabla u|)\nabla u \cdot \nabla v \, \mathrm{d}x = \langle f, v\rangle \quad \forall\, v \in H_0^1(D).$

Here, the right-hand side $f$ corresponds to the weak form of

$$f = f_0 + \operatorname{div} M \quad \text{with } M = M_1 \chi_{\Omega_{\mathrm{ma}}}(x) + M_2 \chi_{D\setminus\Omega_{\mathrm{ma}}}(x)$$

as in section 5, where $f_0 = J_i$, $M_1 = -\frac{\nu}{\nu_0}\binom{-M_y}{M_x}$ and $M_2 = 0$. The vector $\binom{M_x}{M_y}$ denotes the permanent magnetization of the magnets. It is a constant vector in each of the magnet subdomains pointing in the directions indicated in Figure 1, and it vanishes outside the magnet areas. The function $J_i$ represents the impressed currents in the coil areas $\Omega_{\mathrm{c}}$ (light blue areas in Figure 1) and is assumed to vanish in this special application, i.e., $J_i = 0$. The right-hand side $f \in H^{-1}(D)$ reads

$$\langle f, v\rangle = \int_D J_i\, v \,-\, M_1 \cdot \nabla v \,\mathrm{d}x = -\int_{\Omega_{\mathrm{ma}}} M_1 \cdot \nabla v \,\mathrm{d}x. \tag{6.2}$$

We consider admissible shapes $\Omega \in \mathcal{O}$ as in (2.5) and in section 5. Furthermore,

$$\nu(x, |\nabla u|) = \chi_{\Omega_f}(x)\, \hat{\nu}(|\nabla u|) + \chi_{D\setminus\Omega_f}(x)\, \nu_0$$

denotes the magnetic reluctivity composed of a nonlinear function $\hat{\nu}$ depending on the magnitude of the magnetic flux density $|B| = |\nabla u|$ inside the ferromagnetic material and a constant $\nu_0 = 10^7/(4\pi)$, which is expressed in the unit $m\, kg\, A^{-2}\, s^{-2}$, otherwise. The constant $\nu_0$ is the magnetic reluctivity of vacuum which is practically the same as that of air. The nonlinear function $\hat{\nu}$ is in practice obtained from measurements and is not available in a closed form. However, the physical properties of magnetic fields yield the following characteristics of $\hat{\nu}$:

(i) $\hat{\nu}$ is continuously differentiable on $(0, \infty)$;
(ii) $\exists\, m > 0 :\ \hat{\nu}(s) \geq m$ for all $s \in \mathbb{R}_0^+$;
(iii) $\hat{\nu}(s) \leq \nu_0$ for all $s \in \mathbb{R}_0^+$;
(iv) $(\hat{\nu}(s)s)' = \hat{\nu}(s) + \hat{\nu}'(s)s \geq m > 0$;
(v) $s \mapsto \hat{\nu}(s)s$ is strongly monotone with monotonicity constant $m$, i.e.,

$$(\hat{\nu}(s)\, s - \hat{\nu}(t)\, t)\, (s - t) \geq m(s - t)^2 \quad \forall\ s, t \geq 0;$$

(vi) $s \mapsto \hat{\nu}(s)s$ is Lipschitz continuous with Lipschitz constant $\nu_0$, i.e.,

$$|\hat{\nu}(s)\, s - \hat{\nu}(t)\, t| \leq \nu_0 |s - t| \quad \forall\ s, t \geq 0.$$

For more details on properties and practical realization of the function $\hat{\nu}$ from given measurement data, we refer the reader to [19, 29, 43].

In order to be able to apply Theorem 5.1 to the problem above, we have to check whether Assumption 1 is satisfied for

$$\beta_1(\zeta) := \hat{\nu}(\sqrt{\zeta}) \quad \text{and} \quad \beta_2(\zeta) := \nu_0.$$

Clearly, all four conditions of Assumption 1 are fulfilled for $\beta_2(\zeta) = \nu_0 = \text{const}$. Now let us more closely investigate $\beta_1$. Notice the relations $\beta_1(|\rho|^2) = \hat{\nu}(|\rho|)$ and $\beta_1'(|\rho|^2) = \hat{\nu}'(|\rho|)/(2|\rho|)$.

1. As mentioned above, the function $\hat{\nu}$ is bounded from above by the magnetic reluctivity of vacuum $\nu_0$ and from below by a positive constant $m$; cf. Figure 2(a).
2. Assumption 1(2) holds for the function $\hat{\nu}$ by virtue of properties (v) and (vi).

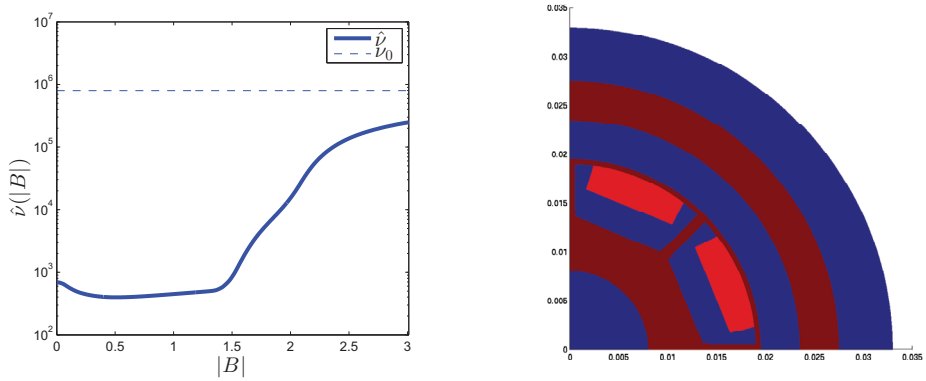


(a) (b)

FIG. 2. (a) *Magnetic reluctivity $\hat{\nu}$ as a function of the magnitude $|B| = |\nabla u|$ of the magnetic flux density.* (b) *Ferromagnetic material $\Omega_f$ with design subdomains $\Omega \subset \Omega_f$ (highlighted).*

3. The numerical realization of the function $\hat{\nu}$ consists of an interproximation of given measurement data (see [29]). The interproximation was done using splines of class $C^1$.
4. It is easy to see that this condition for $\beta_1$ is equivalent to

$$\exists \lambda,\, \Lambda > 0 : \lambda|\eta|^2 \le \eta^T \left(\beta_1(|\rho|^2) I_2 + 2\beta_1'(|\rho|^2)\rho \otimes \rho\right) \eta \le \Lambda|\eta|^2$$

or, in terms of $\hat{\nu}$,

$$\exists \lambda,\, \Lambda > 0 : \lambda|\eta|^2 \le \eta^T \left(\hat{\nu}(|\rho|) I_2 + \frac{\hat{\nu}'(|\rho|)}{|\rho|}\rho \otimes \rho\right) \eta \le \Lambda|\eta|^2,$$

where $I_2$ denotes the identity matrix of dimension 2. The eigenvalues and corresponding eigenvectors of the $2 \times 2$ matrix $\hat{\nu}(|\rho|)I_2 + \frac{\hat{\nu}'(|\rho|)}{|\rho|}\rho \otimes \rho$ are given by

$$\lambda_1 = \hat{\nu}(|\rho|), \qquad v_1 = \begin{pmatrix} -\rho_2 \\ \rho_1 \end{pmatrix},$$
$$\lambda_2 = \hat{\nu}(|\rho|) + \hat{\nu}'(|\rho|)|\rho|, \qquad v_2 = \begin{pmatrix} \rho_1 \\ \rho_2 \end{pmatrix}.$$

From the physical properties (ii) and (iv) of $\hat{\nu}$, it follows that both $\lambda_1$ and $\lambda_2$ are positive. Therefore, the assumption holds with $\lambda = \min\{\lambda_1, \lambda_2\}$ and $\Lambda = \max\{\lambda_1, \lambda_2\}$.

Properties (v) and (vi), together with Assumption 1(1), yield existence and uniqueness of a solution $u \in H_0^1(D)$ to the state equation. Assumption 1(4) ensures the existence and uniqueness of an adjoint state $p \in H_0^1(D)$.

Thus, we can apply Theorem 5.1, and the shape derivative is given by (5.1).

**6.1. Numerical method.** In each iteration of the optimization process, we use the shape derivative $dJ(\Omega; V)$ derived in (5.1) to compute a vector field $V$ that ensures a decrease of the objective function $dJ(\Omega; V) \le 0$ by displacing the interface between the iron subdomain $\Omega$ and the air subdomain $\Omega^{\text{ref}} \setminus \Omega$ along that vector field.

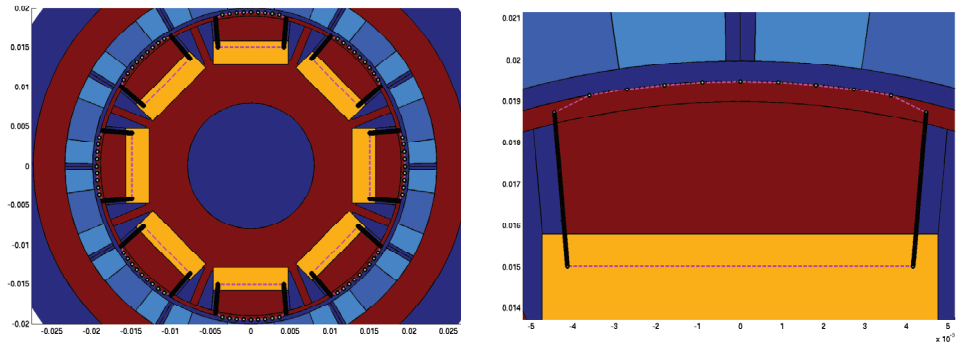

(a) (b)

FIG. 3. (a) *Interface points around eight design areas of the electric motor.* (b) *Zoom on the upper design area: Fictitious interface polygon consists of* 151 *points (*71 *on the left,* 71 *on the right, and* 9 *on top).*

**6.1.1. Setup of interface.** Due to practical restrictions, we choose not to move the interface by moving the single points of the mesh, as it is common practice in shape optimization. Instead, we model the interface by setting up a polygon with 151 points around each of the design subdomains $\Omega_k^{ref}$ (see Figure 3) and move the points of these polygons along the calculated velocity field $V$ in the course of the optimization process. Each element of the design area whose center of gravity is inside this polygon is considered to be ferromagnetic material, while the others are considered to be air. That way, we can avoid problems such as deformation of the fixed parts of the motor, i.e., magnets or the air gap, or self-intersections of the mesh.

**6.1.2. Descent direction.** In order to get a descent in the cost functional, we compute the velocity field as follows. We choose a symmetric and positive definite bilinear form

$$b : H_0^1(D_{\text{rot}}) \times H_0^1(D_{\text{rot}}) \to \mathbb{R}$$

defined on the subdomain $D_{\text{rot}}$ of $D$ representing the rotor and compute $V$ as the solution of the following variational problem:

$$\text{Find } V \in P_h \quad \text{such that } b(V, W) = -dJ(\Omega, W) \quad \forall\, W \in P_h, \tag{6.3}$$

where $P_h \subset H_0^1(D_{\text{rot}})$ is a finite-dimensional subspace. Outside $D_{\text{rot}}$ we extend $V$ by zero. Note that, by this choice, the condition $V = 0$ on $\Gamma_0$, which is assumed in section 5, is satisfied. The obtained descent directions $V \in P_h$ will also be in $W^{1,\infty}(D, \mathbf{R}^2)$, and, consequently, they are admissible vector fields defining a flow $T_t^V$. The solution $V$ computed this way is a descent direction for the cost functional since

$$dJ(\Omega, V) = -b(V, V) \leq 0.$$

For our numerical experiments, we choose the bilinear form

$$\begin{aligned} &b : H_0^1(D_{\text{rot}}) \times H_0^1(D_{\text{rot}}) \to \mathbb{R}, \\ &b(V, W) = \int_{D_{\text{rot}}} (\alpha\, \mathrm{D}V : \mathrm{D}W + V \cdot W)\, \mathrm{d}x. \end{aligned} \tag{6.4}$$

Here, the penalization function $\alpha \in L^\infty(D_{\mathrm{rot}})$ is chosen as

$$\alpha(x) = \begin{cases} 1, & x \in \Omega, \\ 10, & x \in \Omega^\varepsilon \setminus \Omega, \\ 10^2, & \text{else}, \end{cases}$$

where $\Omega^\varepsilon = \{x \in D_{\mathrm{rot}} : \mathrm{dist}(x, \Omega) \leq \varepsilon\}$ for some small $\varepsilon > 0$. With this choice of $\alpha$, we ensure that the resulting velocity field $V$ is small outside the design region $\Omega^{\mathrm{ref}}$.

We remark that the numerical overhead of using the volume form of the shape derivative compared to Hadamard's boundary-based form is the solution of the auxiliary boundary value problem (6.4). However, the additional numerical effort of solving this linear boundary value problem is negligible compared to the effort of solving the nonlinear state equation (2.1). Furthermore, we solve this problem only on the reduced computational domain $D_{\mathrm{rot}} \subset D$.

For all numerical simulations, we used piecewise linear finite elements on a triangular grid with 44810 degrees of freedom and 89454 elements, where we chose a particularly fine discretization in the design regions $\Omega^{\mathrm{ref}}$ (53488 design elements). The nonlinear state equation (2.1) is solved by Newton's method. All arising linear systems of finite element equations are solved using the parallel direct solver PARDISO [15].

**6.1.3. Updating the interface.** For updating the interface, we perform a backtracking (line search) algorithm: Once a descent direction $V$ is computed, we move all interface points a step size $\tau = \tau_{init}$ in the direction given by $V$ and evaluate the cost function for the updated geometry. If the cost value has not decreased, the step size $\tau$ is halved and the cost function is evaluated for the new, updated geometry. We repeat this step until a decrease of the cost function is achieved. When the step size becomes too small such that no element switches its state, the algorithm is stopped.

**6.2. Numerical results.** The procedure is summarized in Algorithm 1.

ALGORITHM 1. *Set converged = false*
*While converged == false*

1. *Compute state u using* (2.1) *and adjoint state p using* (4.11).
2. *Compute descent direction V using* (6.3) *with* $dJ(\Omega; V)$ *given in* (5.1).
3. *Find step width* $\tau$ *that yields a decrease in the cost function using backtracking.*
4. *If decrease in the cost function could be achieved:*
   *Update interface and go to step* 1.

   *else:*
   *converged = true.*

The final design after 35 iterations of Algorithm 1 can be seen in Figure 4. The cost function is reduced from $1.3033 * 10^{-3}$ to $0.94997 * 10^{-3}$, i.e., by about 27% (see Figure 5(a)). As a measure of optimality of the final design, we observed the norm of the gradient of the Lagrangian, which amounts to the shape derivative $dJ(\Omega; V)$ of the cost functional. We observed a decrease of this quantity from 0.059985 to 0.033305. A further decrease of the shape gradient could be achieved by using a finer grid. We note that our approach of updating the interface does not allow for arbitrarily small changes of the geometry, and therefore the gradient of the Lagrangian does not vanish for our final design. An incorporation of a nonstandard finite element method to accurately resolve the interface while keeping the mesh fixed is a subject of ongoing studies. The radial component of the magnetic field on the circle $\Gamma_0$ in the air gap for the initial (blue), desired (green), and final design (red) can be seen in Figure 5(b). The optimization process took about 26 minutes using a single core on a laptop.

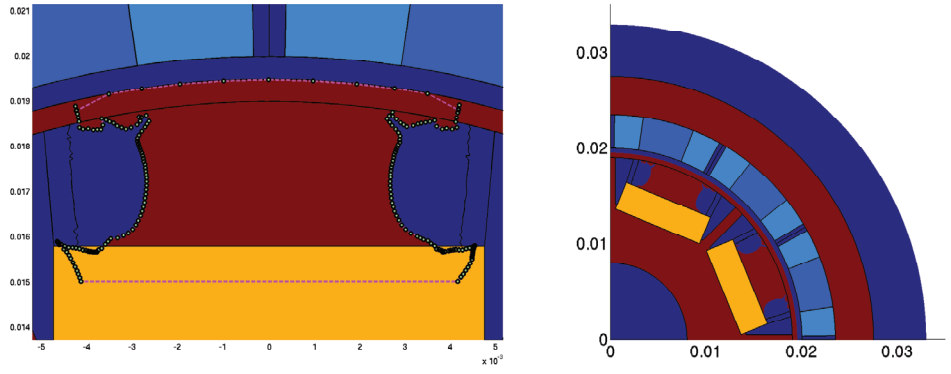


(a) (b)

FIG. 4. (a) *Final design of one component* $\Omega_k$ *after* 35 *iterations of Algorithm* 1. (b) *Upper-right quarter of the optimized motor.*

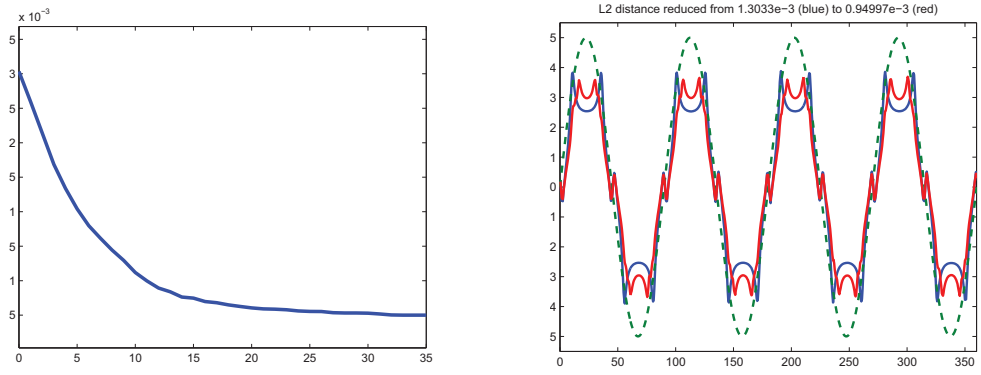


(a) (b)

FIG. 5. (a) *Decrease of cost functional in the course of the optimization process.* (b) *Radial component of the magnetic flux density* $B$ *along curve* $\Gamma_0$ *in the air gap: initial design (blue), desired sine curve* $B_d$ *(green), and final (red) design.*

**7. Conclusion and outlook.** In this paper, we have performed the rigorous analysis of the shape sensitivity analysis of a subregion $\Omega$ of the rotor of an electric motor in order to match a certain rotation pattern. The shape derivative of the cost functional was computed efficiently using a shape-Lagrangian method for nonlinear partial differential equation constraints that allows us to bypass the computation of the material derivative of the state. The implementation of the obtained shape derivative in a numerical algorithm provides an interesting shape, which allows us to improve the rotation pattern. In the numerical experiment presented in this work, we chose a rather simple way of updating the interface: We just switched the state of single elements of the finite element mesh from one material to the other. For a more accurate resolution of the interface, one may employ a nonstandard finite element method, such as the extended finite element method (XFEM) [40] or the immersed FEM [37], or a discontinuous Galerkin approach based on Nitsche's idea; see [16].

These approaches make it possible to represent, without loss of accuracy, an interface that is not aligned with the underlying finite element discretization. An alternative way to achieve this would be to locally modify the finite element basis in a parametric way as it is done in [11].

**Acknowledgments.** The first and second authors thank the Linz Center of Mechatronics (LCM) for supporting their work on topology and shape optimization of electrical machines.

REFERENCES

[1] S. Amstutz and A. Laurain, *A semismooth Newton method for a class of semilinear optimal control problems with box and volume constraints*, Comput. Optim. Appl., 56 (2013), pp. 369–403.

[2] R. Arumugam, J. Lindsay, D. Lowther, and R. Krishnan, *Magnetic field analysis of a switched reluctance motor using a two dimensional finite element model*, IEEE Trans. Magn., 21 (1985), pp. 1883–1885.

[3] M. Berggren, *A unified discrete-continuous sensitivity analysis method for shape optimization*, in Applied and Numerical Partial Differential Equations, Comput. Methods Appl. Sci. 15, Springer, New York, 2010, pp. 25–39.

[4] A. Binder, *Elektrische Maschinen und Antriebe: Grundlagen, Betriebsverhalten*, Springer, Heidelberg, 2012.

[5] A. Bonnafé, *Développements asymptotiques topologiques pour une classe d'équations elliptiques quasi-linéaires. Estimations et développements asymptotiques de p-capacités de condensateur. Le cas anisotrope du segment*, Ph.D. thesis, Université de Toulouse, Toulouse, France, 2013.

[6] J. Céa, *Conception optimale ou identification de formes, calcul rapide de la derivee dircetionelle de la fonction cout*, Math. Model. Numer. Anal., 20 (1986), pp. 371–402.

[7] J. Choi, K. Izui, S. Nishiwaki, A. Kawamoto, and T. Nomura, *Rotor pole design of IPM motors for a sinusoidal air-gap flux density distribution*, Structural Multidiscip. Optim., 46 (2012), pp. 445–455.

[8] J. S. Choi, K. Izui, A. Kawamoto, S. Nishiwaki, and T. Nomura, *Topology optimization of the stator for minimizing cogging torque of IPM motors*, IEEE Trans. Magn., 47 (2011), pp. 3024–3027.

[9] M. C. Delfour and J.-P. Zolésio, *Shape sensitivity analysis via min max differentiability*, SIAM J. Control Optim., 26 (1988), pp. 834–862.

[10] M. C. Delfour and J.-P. Zolésio, *Shapes and Geometries. Metrics, Analysis, Differential Calculus, and Optimization*, 2nd ed., Adv. Des. Control 22, SIAM, Philadelphia, 2011.

[11] S. Frei and T. Richter, *A locally modified parametric finite element method for interface problems*, SIAM J. Numer. Anal., 52 (2014), pp. 2315–2334.

[12] G. Frémiot, W. Horn, A. Laurain, M. Rao, and J. Sokołowski, *On the analysis of boundary value problems in nonsmooth domains*, Dissertationes Math. (Rozprawy Mat.), 462 (2009).

[13] P. Fulmański, A. Laurain, J.-F. Scheid, and J. Sokołowski, *A level set method in shape and topology optimization for variational inequalities*, Int. J. Appl. Math. Comput. Sci., 17 (2007), pp. 413–430.

[14] P. Gangl and U. Langer, *Topology optimization of electric machines based on topological sensitivity analysis*, Comput. Vis. Sci., 15 (2012), pp. 345–354.

[15] K. Gartner and O. Schenk, *Solving unsymmetric sparse systems of linear equations with PARDISO*, J. Future Generation Comput. Systems, 20 (2004), pp. 475–487.

[16] A. Hansbo and P. Hansbo, *An unfitted finite element method, based on Nitsche's method, for elliptic interface problems*, Comput. Methods Appl. Mech. Engrg., 191 (2002), pp. 5537–5552.

[17] J. Haslinger and R. A. E. Mäkinen, *Introduction to Shape Optimization: Theory, Approximation, and Computation*, Adv. Des. Control 7, SIAM, Philadelphia, 2003.

[18] J. Haslinger and P. Neittaanmäki, *Finite Element Approximation for Optimal Shape, Material and Topology Design*, 2nd ed., John Wiley & Sons, Ltd., Chichester, 1996.

[19] B. Heise, *Analysis of a fully discrete finite element method for a nonlinear magnetic field problem*, SIAM J. Numer. Anal., 31 (1994), pp. 745–759.

[20] A. Henrot and M. Pierre, *Variation et optimisation de formes. Une analyse géométrique,* Math. Appl. 48, Springer, Berlin, 2005.
[21] M. Hintermüller and A. Laurain, *A shape and topology optimization technique for solving a class of linear complementarity problems in function space*, Comput. Optim. Appl., 46 (2010), pp. 535–569.
[22] M. Hintermüller and A. Laurain, *Optimal shape design subject to elliptic variational inequalities*, SIAM J. Control Optim., 49 (2011), pp. 1015–1047.
[23] R. Hiptmair, A. Paganini, and S. Sargheini, *Comparison of approximate shape gradients*, BIT, 55 (2015), pp. 459–485.
[24] J.-P. Hong, J. Kwack, and S. Min, *Optimal stator design of interior permanent magnet motor to reduce torque ripple using the level set method*, IEEE Trans. Magn., 46 (2010), pp. 2108–2111.
[25] M. Iguernane, S. A. Nazarov, J.-R. Roche, J. Sokolowski, and K. Szulc, *Topological derivatives for semilinear elliptic equations*, Int. J. Appl. Math. Comput. Sci., 19 (2009), pp. 191–205.
[26] K. Ito, K. Kunisch, and Z. Li, *Level-set function approach to an inverse interface problem*, Inverse Problems, 17 (2001), pp. 1225–1242.
[27] K. Ito, K. Kunisch, and G. H. Peichl, *Variational approach to shape derivatives*, ESAIM Control Optim. Calc. Var., 14 (2008), pp. 517–539.
[28] M. Jung and U. Langer, *Methode der finiten Elemente für Ingenieure: Eine Einführung in die numerischen Grundlagen und Computersimulation*, Springer-Vieweg–Verlag, Darmstadt, 2013.
[29] B. Jüttler and C. Pechstein, *Monotonicity-preserving interproximation of B-H-curves*, J. Comput. Appl. Math., 196 (2006), pp. 45–57.
[30] H. Kasumba and K. Kunisch, *On shape sensitivity analysis of the cost functional without shape sensitivity of the state variable*, Control Cybernet., 40 (2011), pp. 989–1017.
[31] H. Kasumba and K. Kunisch, *On computation of the shape Hessian of the cost functional without shape sensitivity of the state variable*, J. Optim. Theory Appl., 162 (2014), pp. 779–884.
[32] J. Kolota and S. Steien, *Analysis of 2D and 3D finite element approach of a switched reluctance motor*, Przegląd Elektrotechniczny (Elec. Rev.), 87 (2011), pp. 188–190.
[33] E. Laporte and P. L. Tallec, *Numerical Methods in Sensitivity Analysis and Shape Optimization*, Model. Simul. Sci. Eng. Technol., Birkhäuser Boston, Inc., Boston, MA, 2003.
[34] A. Laurain, *Global minimizer of the ground state for two phase conductors in low contrast regime*, ESAIM Control Optim. Calc. Var., 20 (2014), pp. 362–388.
[35] A. Laurain, M. Hintermüller, M. Freiberger, and H. Scharfetter, *Topological sensitivity analysis in fluorescence optical tomography*, Inverse Problems, 29 (2013), 025003.
[36] A. Laurain and K. Sturm, *Distributed shape derivative via averaged adjoint method and applications*, ESAIM Math. Model. Numer. Anal., to appear. doi:10.1051/m2an/2015075.
[37] Z. Li, T. Lin, and X. Wu, *New Cartesian grid methods for interface problems using the finite element formulation*, Numer. Math., 96 (2003), pp. 61–98.
[38] D. Miyagi, S. Shimose, N. Takahashi, and T. Yamada, *Optimization of rotor of actual IPM motor using ON/OFF method*, IEEE Trans. Magn., 47 (2011), pp. 1262–1265.
[39] D. Miyagi, N. Takahashi, and T. Yamada, *Examination of optimal design on IPM motor using ON/OFF method*, IEEE Trans. Magn., 46 (2010), pp. 3149–3152.
[40] N. Mos, J. Dolbow, and T. Belytschko, *A finite element method for crack growth without remeshing*, Int. J. Numer. Methods Engrg., 46 (1999), pp. 131–150.
[41] A. A. Novotny and J. Sokołowski, *Topological Derivatives in Shape Optimization*, Interact. Mech. Math., Springer, Heidelberg, 2013.
[42] O. Pantz, *Sensibilité de l'équation de la chaleur aux sauts de conductivité*, C. R. Math. Acad. Sci. Paris, 341 (2005), pp. 333–337.
[43] C. Pechstein, *Multigrid-Newton-Methods for Nonlinear Magnetostatic Problems*, Master's thesis, Johannes Kepler University Linz, Linz, Austria, 2004.
[44] C. Pechstein, *Finite and Boundary Element Tearing and Interconnecting Methods for Multiscale Elliptic Partial Differential Equations*, Ph.D. thesis, Johannes Kepler University Linz, Linz, Austria, 2008.
[45] O. Pironneau, *Optimal Shape Design for Elliptic Systems*, Springer Ser. Comput. Phys., Springer-Verlag, New York, 1984.
[46] S. Schmidt, C. Ilic, V. Schulz, and N. Gauger, *Three-dimensional large-scale aerodynamic shape optimization based on shape calculus*, AIAA J., 51 (2013), pp. 2615–2627.
[47] J. Sokołowski and A. Żochowski, *On the topological derivative in shape optimization*, SIAM J. Control Optim., 37 (1999), pp. 1251–1272.

[48] J. Sokołowski and J.-P. Zolésio, *Introduction to Shape Optimization. Shape Sensitivity Analysis*, Springer Ser. Comput. Math. 16, Springer-Verlag, Berlin, 1992.

[49] K. Sturm, *Minimax Lagrangian approach to the differentiability of nonlinear PDE constrained shape functions without saddle point assumption,* SIAM J. Control Optim., 53 (2015), pp. 2017–2039. doi:10.1137/130930807.

[50] H. Torkaman and E. Afjei, *Comprehensive study of* 2-*D and* 3-*D finite element analysis of a switched reluctance motor*, J. Appl. Sci., 8 (2008), pp. 2758–2763.

[51] G. Weidenholzer, S. Silber, G. Jungmayr, G. Bramerdorfer, H. Grabner, and W. Amrhein, *A flux-based PMSM motor model using RBF interpolation for time-stepping simulations*, in Proceedings of the 2013 IEEE International Electric Machines & Drives Conference (IEMDC), Chicago, IL, 2013, pp. 1418–1423.

[52] E. Zeidler, *Applied Functional Analysis: Applications to Mathematical Physics*, Appl. Math. Sci. 108, Springer, New York, 1995.